





## ARTICLE

# Integrated systems modeling of severe asthma: Exploration of IL-33/ST2 antagonism

Kapil Gadkar<sup>1</sup> | Justin Feigelman<sup>1</sup>  | Siddharth Sukumaran<sup>1</sup> | Manoj C. Rodrigo<sup>1</sup> | Tracy Staton<sup>1</sup>  | Fang Cai<sup>1</sup> | Rebecca N. Bauer<sup>1</sup> | David F. Choy<sup>1</sup>  | Cynthia L. Stokes<sup>2</sup> | Heleen Scheerens<sup>1</sup> | Saroja Ramanujan<sup>1</sup> 

<sup>1</sup>Genentech, Inc., South San Francisco, California, USA

<sup>2</sup>Stokes Consulting, Redwood City, California, USA

**Correspondence**

Saroja Ramanujan, Genentech, Inc, 1 DNA Way, South San Francisco, CA 94080, USA.

Email: [ramanujan.saroja@gene.com](mailto:ramanujan.saroja@gene.com)

**Present address**

Kapil Gadkar, Denali Therapeutics, Inc., South San Francisco, California, USA

Siddharth Sukumaran, Janssen, Inc., Spring House, Pennsylvania, USA

Manoj C. Rodrigo, Stryker, Inc., Fremont, California, USA

Fang Cai, AbbVie, Inc., South San Francisco, California, USA

**Funding information**

No funding was received for this work

**Abstract**

Asthma is a complex, heterogeneous disease with a high unmet medical need, despite therapies targeting a multitude of pathways. The ability to quantitatively integrate preclinical and clinical data on these pathways could aid in the development and testing of novel targets and therapeutics. In this work, we develop a computational model of asthma biology, including key cell types and mediators, and create a virtual population capturing clinical heterogeneity. The simulated responses to therapies targeting IL-13, IL-4R $\alpha$ , IL-5, IgE, and TSLP demonstrate agreement with clinical endpoints and biomarkers of type 2 (T2) inflammation, including blood eosinophils, FEV1, IgE, and FeNO. We use the model to explore the potential benefit of targeting the IL-33 pathway with anti-IL-33 and anti-ST2. Model predictions are compared with data on blood eosinophils, FeNO, and FEV1 from recent anti-IL-33 and anti-ST2 trials and used to interpret trial results based on pathway biology and pharmacology. Results of sensitivity analyses on the contributions of IL-33 to the predicted biomarker changes suggest that anti-ST2 therapy reduces circulating blood eosinophil levels primarily through its impact on eosinophil progenitor maturation and IL-5-dependent survival, and induces changes in FeNO and FEV1 through its effect on immune cells involved in T2 cytokine production. Finally, we also investigate the impact of ST2 genetics on the conferred benefit of anti-ST2. The model includes representation of a wide array of biologic mechanisms and interventions that will provide mechanistic insight and support clinical program design for a wide range of novel therapies during drug development.

Kapil Gadkar and Justin Feigelman contributed equally to this work.

This is an open access article under the terms of the [Creative Commons Attribution-NonCommercial](https://creativecommons.org/licenses/by-nc/4.0/) License, which permits use, distribution and reproduction in any medium, provided the original work is properly cited and is not used for commercial purposes.

© 2022 Genentech Inc. *CPT: Pharmacometrics & Systems Pharmacology* published by Wiley Periodicals LLC on behalf of American Society for Clinical Pharmacology and Therapeutics.

## Study Highlights

### WHAT IS THE CURRENT KNOWLEDGE ON THE TOPIC?

The IL-33/ST2 pathway contributes to activation of immune cells and may contribute to asthma exacerbation. Phase II trials of anti-IL-33 therapy demonstrated increases in FEV1 and decreases in blood eosinophils, whereas anti-ST2 therapy demonstrated a decreased rate of exacerbation.

### WHAT QUESTION DID THIS STUDY ADDRESS?

This work investigates the IL-33/ST2 pathway using computational modeling to predict biomarker changes and provide insights into the respective contributions of multiple inflammatory pathways toward relevant clinical end points.

### WHAT DOES THIS STUDY ADD TO OUR KNOWLEDGE?

This computational model developed includes multiple highly relevant pathways, cell types, and therapies. Analysis reveals a disconnect between the observed effects of anti-IL-33 versus anti-ST2, and suggests that non-type 2 biology may significantly contribute to the clinical response of ST2 inhibition, highlighting the need for further investigations into these mechanisms.

### HOW MIGHT THIS CHANGE DRUG DISCOVERY, DEVELOPMENT, AND/OR THERAPEUTICS?

The model will be used for continuing support of multiple therapeutics through in silico investigations to support trial design, assess relative importance of associated pathways, and better understand the mechanistic origins of clinical phenotypes of interest.

## INTRODUCTION

Asthma is a heterogeneous disease with a high unmet medical need. The type 2 (T2) high variety is clinically distinguished by eosinophilia and the elevation of T2 cytokines, including IL-5, IL-4, and IL-13,<sup>1</sup> which regulate eosinophils,<sup>2</sup> B cells,<sup>3</sup> airway constriction, and NO production.<sup>4</sup> Conversely, T2 low asthma is characterized by reduced T2 cytokines, FeNO, blood eosinophils, and IgE.<sup>5</sup> T2 low asthma remains poorly understood but may be associated with IL-17, or TNF- $\alpha$ , and other clinical phenotypes, such as obesity-dependent or pauci-granulocytic asthma.<sup>5,6</sup> Although much is known about asthma etiology, accurate prediction of clinical efficacy of novel therapeutics remains a challenging task.

The alarmin IL-33 may play a central role in asthma exacerbation. It is released by airway epithelial cells in response to cigarette smoke, allergens, and viruses, and drives inflammatory processes in cells that expressing the ST2 receptor. Inhibition of the IL-33 pathway promotes Th1 responses while reducing Th2 activity in vitro and in rodent models,<sup>7</sup> whereas administration of IL-33 upregulates T2 cytokines in ST2-expressing cells. ST2 inhibition may therefore impact T2-associated clinical endpoints and reduce exacerbation rates. This hypothesis was recently confirmed in the Zenyatta phase II clinical trial of the anti-ST2 molecule astegolimab, with significant reductions observed in exacerbations in both eosinophil high and low

populations<sup>8</sup> (see e.g., ref. 9 for an overview of recent and ongoing clinical investigations).

The focus of the current work is to explore in silico the effects of several therapies and to predict the efficacy of anti-IL-33 and anti-ST2 therapy for a severe asthmatic population. We compare these predictions with recent clinical data and explore the impact of IL-33/ST2 pathway associated biology. To do this we utilize a quantitative systems pharmacology (QSP) model of asthma (see e.g., ref. 10 for an overview of QSP model application). Our model is more expansive than previous models that either focused on eosinophil hematopoiesis and trafficking,<sup>11</sup> the regulation of leukotriene and 5-lipoxygenase inhibitors,<sup>12</sup> or the role of DP<sub>2</sub>.<sup>13</sup> An early disease model predicted initial failures of non-stratified anti-IL-5 trials,<sup>14</sup> but does not include recent targets, such as TSLP or IL-33. Ongoing clinical development, such as the approval of mepolizumab in 2015, dupilumab in 2018, tezepelumab in 2021, and the investigation of anti-ST2 and anti-IL-33, highlight the need for QSP models that holistically integrate newer therapies and pathways beyond IL-5/IL-13.

Our model captures the cellular effect of therapies and subsequent impact on clinical end points, including FeNO (a marker of T2 inflammation<sup>15</sup>), eosinophils (which may directly contribute to asthma severity<sup>16</sup>), and FEV1 (a measure of airway function), for severe, uncontrolled asthma. Calibration is verified using data from therapies targeting IL-5, IL-13, IL-4R $\alpha$ , TSLP, and IgE, and further

validated against held-out anti-TSLP data. We then predict the impact of inhibition of IL-33 (etokimab) and validate against recent studies of monotherapy anti-IL-33 or combination with anti-IL-4R $\alpha$  (dupixent, REGN-3500). Using the validated model, we predict the outcome of anti-ST2 therapy with astegolimab and compare with results from the Zenyatta phase IIb trial.<sup>8</sup> We further predict the impact of a genetic variant associated with reduced IL-33 activity. Last, we perform sensitivity analyses to investigate the role of IL-33-dependent pathways in driving biomarker changes. In total, our model provides mechanistic insights into multiple T2-dependent pathways and in particular provides the basis for a quantitative understanding of the role of IL-33/ST2 biology in severe asthma.

## METHODS

The model represents cells and mediator molecules within physiological components, including airway wall tissue, smooth muscle, peripheral circulation, and bone marrow. Model components and interactions are illustrated in Figure 1 and summarized in Tables S1 and S2. A detailed description of biological modules and pharmacokinetics are presented in the [Supplementary Information](#). The model was developed using the Simbiology Toolbox in MATLAB (Mathworks) and gQSPSim.<sup>17</sup> All model equations, rules, and reactions can be found in the [Supplementary Excel tables](#).

### Reference subject and virtual populations

Model development followed our previously described general QSP workflow.<sup>18</sup> After biological scoping and

model construction, a “reference patient” was developed that matches the average of the clinical data at each timepoint for multiple therapies. We then developed a virtual population (Vpop) based on the population of the LAVOLTA I/II clinical trials of lebrikizumab in patients with severe asthma,<sup>19</sup> matching baseline and response to therapy. The Vpop was subdivided as in LAVOLTA into eosinophil high (>300 cells/ $\mu$ l) and low ( $\leq$ 300 cells/ $\mu$ l) subpopulations, based on blood levels prior to therapy. These populations differ in baseline eosinophils, Th2s, and B cells, overall T2 inflammation (including IL-4, IL-13, and IL-5 levels), and airway smooth muscle layer thickness. Model parameters used in the Vpop are shown in Table S3. The Vpop development process is described in more detail in the [Supplementary Information](#).

### Pharmacokinetics of therapeutics

Pharmacokinetic (PK) models for each therapy were built using published data or derived from established PK/pharmacodynamic (PD) models, see [Supplementary Information](#) for details. We are primarily interested in understanding the heterogeneous response in the Vpop due to population variability. Thus, we do not explore variability in PK in the present work.

## RESULTS

### Reference patient calibration

The reference patient was calibrated to be consistent with data for patients with severe asthma on inhaled

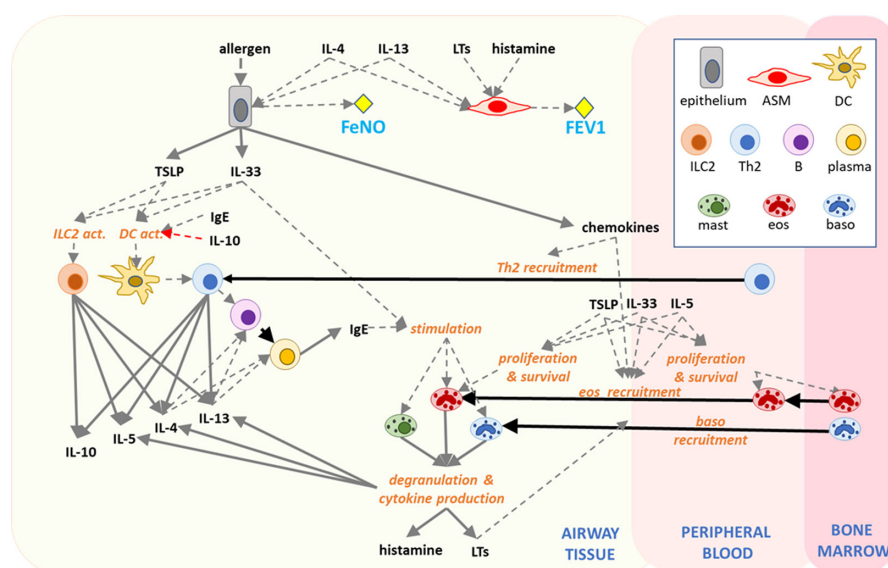
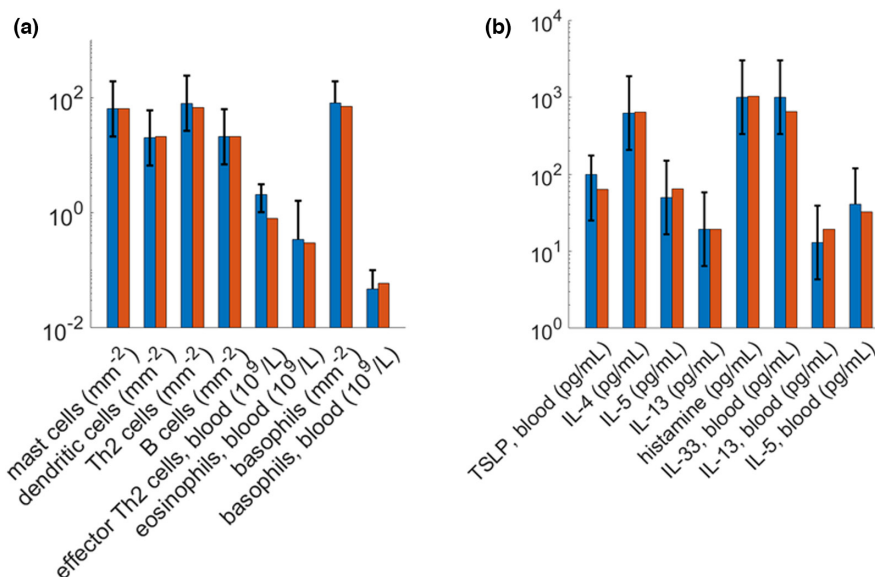


**FIGURE 1** The asthma QSP model captures numerous immune cell components across tissue compartments, including airway wall, circulation, and the bone marrow. Effects such as proliferation, recruitment, and activation of immune cells are regulated by diffusing mediators including cytokines, chemokines, and granulocyte products. QSP, quantitative systems pharmacology.

**FIGURE 2** Comparison of biomarker clinical data (blue) with reference patient simulation (red) for severe asthmatic individuals on ICS and LABA background therapy shown for (a). cellular abundances and (b). mediator molecules. Error bars represent the range of observed data if available, otherwise mean  $\pm 2$  standard deviations; simulations represent a single simulated reference patient and have no error bars. Numerical values and units are shown in Table S5. ICS, inhaled corticosteroids; LABA, long-acting  $\beta 2$  agonist.



corticosteroids (ICS) and long-acting  $\beta 2$  agonist (LABA). The clinical data used in calibration, model verification, and validation are captured in Table S4. Model simulations generally capture reference data at baseline for cells (Figure 2a) and mediators (Figure 2b); for data and units see Table S5. Percent change from baseline are also captured, see Figure S1. Together, these results establish that the model details and representation are sufficient to quantitatively capture relevant clinical data.

## Virtual population development and validation

The severe asthma Vpop captures essential biomarkers including blood eosinophils, FeNO, FEV1, and IgE, which reflect different disease axes and which respond to different therapies. Thus, capturing and predicting clinical responses for these biomarkers lends confidence to the robustness of the underlying biological implementation.

We simulated anti-IL-13 treatment dosed at 37.5 and 125 mg, s.c. Q4W. Simulated baseline blood eosinophils, FeNO, FEV1, and IgE are compared with data in Figure 3a–d for the two severe subpopulations; additional biomarkers are shown in Figure S2. T2 cytokines including IL-4, IL-5, and IL-13 are lower in the eosinophil low population, whereas IL-33 and TSLP levels are comparable between the subpopulations. FeNO and IgE levels are lower for the eosinophil low subpopulation in both data and simulations. Biomarker changes are compared in Figure 3e–h. All clinical biomarker changes were placebo subtracted. The Vpop captures the dose-dependent increase in blood eosinophils, especially in the eosinophil high subpopulation, and dose-dependent improvement in

FeNO, FEV1, and IgE. Additional biomarker changes are shown in Figure S3.

The Vpop was further validated for therapies with distinct targets, including IL-5, IL-4R $\alpha$ , IgE, and TSLP. The simulated Vpops are matched to the corresponding trial(s) and compared with clinical data, summarized in Table S4. Due to differences among trial populations, we compare relative changes rather than absolute values. Simulations generally agree with data for blood eosinophils, FeNO, and FEV1, see Figure 4. Simulations were performed using the nonspecific severe Vpop (mepolizumab and omalizumab) or the eosinophil high subpopulation (remaining therapies). Predicted response to anti-TSLP therapy was further validated using the phase IIb PATHWAY trial<sup>20</sup> of tezepelumab, and predicted changes for biomarkers not used in calibration: blood IL-5 decreases 62.6% (–87.0%, –15.0%) versus 65.8% observed, and blood IL-13 decreases 49% (–71.8%, –12.5%) versus 51.7% observed at the administered dose of 210 mg s.c. Q4W.

## Biomarker response to therapies

The model yields insights into biomarker changes and effects in tissues not typically accessible in patients. Biomarker changes for each therapy are summarized in Figure S4.

The model captures clinical data from multiple end points and therapies. For example, eosinophil recruitment is regulated by IL-13 via endothelial adhesion molecule expression<sup>21</sup> and chemokine production. This is captured in the model, and simulations of anti-IL-13 or anti-IL-4R $\alpha$  therapy increase blood eosinophils as was observed clinically.<sup>19</sup> Tissue eosinophils also decrease, consistent with clinical findings.<sup>22</sup> In contrast, simulated anti-IL-5

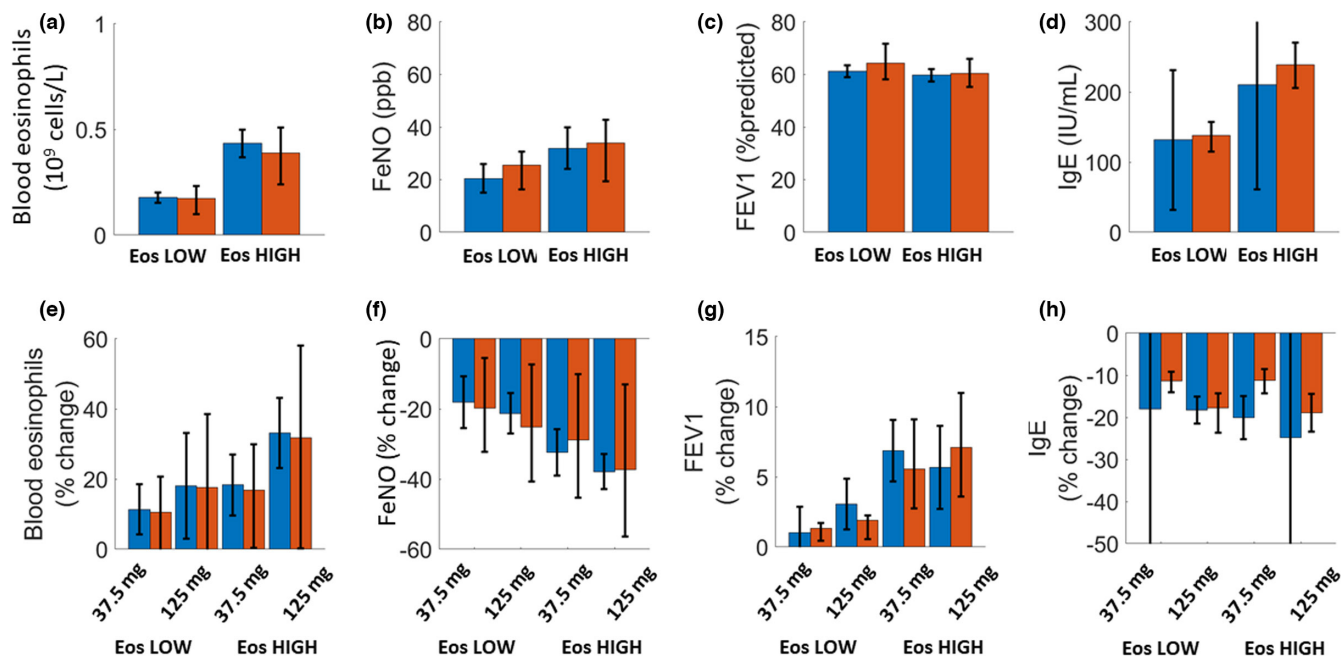


**FIGURE 3** Comparison of clinical data (blue) with the calibrated simulation values (red) for a Vpop based on the LAVOLTA I/II trials of severe asthmatics on ICS and LABA background therapy, treated with lebrikizumab. Simulations and data are shown for eosinophil high and low subpopulations for baseline (a) blood eosinophils, (b) FeNO, (c) FEV1, (d) IgE, and percent change from baseline for (e) blood eosinophils, (f) FeNO, (g) FEV1, and (h) IgE. The mean values are plotted with the middle 50% interval for simulations and standard error for data. EOS, eosinophil; ICS, inhaled corticosteroids; LABA, long-acting  $\beta_2$  agonist; Vpop, virtual population.

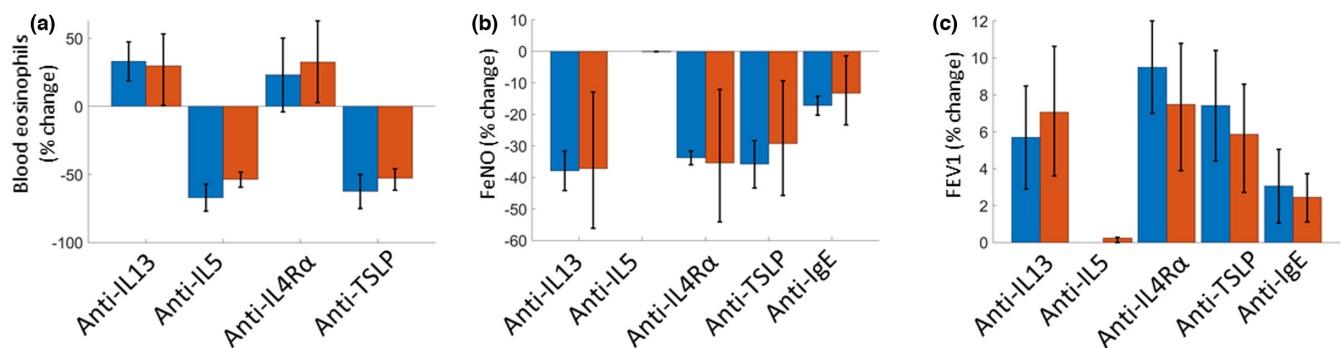


**FIGURE 4** Comparison of treatment effects on percent change from baseline in (a) Blood eosinophils, (b) FeNO, (c) FEV1 in clinical data (blue) and simulated data (red) in the eosinophil high subpopulation. Simulations were performed for high dose anti-IL-13 therapy (lebrikizumab 125 mg Q4W s.c.), anti-IL-5 (mepolizumab 250 mg Q4W i.v.), anti-IL4R $\alpha$  (dupilumab 200 mg Q2W s.c.), anti-TSLP (tezepelumab 280 mg Q2W s.c.), and anti-IgE (90% reduction in IgE). Simulations are shown as time-average mean values and time-average middle 50% interval of the simulation values. Data are shown as mean and standard error.

decreases blood eosinophils, in agreement with clinical observations. TSLP activates production of T2 cytokines and promotes eosinophil proliferation and survival in the bone marrow. Simulated anti-TSLP therapy reduces T2 cytokine production, decreasing recruitment, and reduces eosinophil maturation with an overall net decrease in both tissue and blood eosinophils. Last, anti-IgE therapy reduces Fc $\epsilon$ RI-mediated activation of mast cells and basophils and their production of T2 cytokines. IL-4, IL-13, and IL-5 production all decrease, and the result is a net decrease in blood eosinophils (Figure S1).

Epithelial nitric oxide production is influenced by IL-13 and IL-4.<sup>23,24</sup> Simulated treatment with anti-IL-13, anti-IL-4R $\alpha$ , or anti-TSLP downregulate these pathways, recapitulating the observed drops of 30–40% in FeNO. Anti-IgE therapy reduces FeNO to a lesser degree than therapies directly targeting these pathways. In contrast, anti-IL-5 does not directly affect IL-4 or IL-13 pathways, and anti-IL-5 thus minimally impacts FeNO, as was seen clinically for mepolizumab.

FEV1 is impacted by mediators of bronchoconstriction such as IL-13, IL-4, histamine, or leukotrienes.

Simulations of anti-IL-13, anti-IL-4R $\alpha$ , and anti-TSLP lead to significant increases in FEV1, see [Figure 4c](#). Whereas simulated anti-IL-5 reduces LT and histamine, it does not significantly improve FEV1 in this population.

As described above, the eosinophil high subpopulation has greater levels of T2 cytokines, eosinophils, and ASM thickness. These differences are reflected in both baseline biomarker levels and response to anti-IL-13 therapy, including stronger decreases in multiple cytokines, chemokines and tissue eosinophils, and greater increases in blood eosinophils, see [Figure 3](#).

## Simulations and predictions for IL-33/ST2 targeted drugs

The model includes the following ST2 pathway effects: regulation of T2-cytokine production by ST2 expressing cells, including basophils, Th2s, mast cells, and ILC2s; proliferation of eosinophils and bone marrow progenitor cells; recruitment of eosinophils; antigen presentation by dendritic cells; and degranulation of basophils, mast cells, and eosinophils. The strengths of IL-33-dependent effects were based on published and internal *in vitro* data (see Supplementary Information). The PK of anti-IL-33 therapy was based on etokimab phase I data.<sup>25</sup> In addition, data from the phase I clinical study of healthy volunteers dosed with the anti-ST2 molecule astegolimab (data not published) were used to inform a PK model for s.c. anti-ST2 therapy. We calibrated the effect of IL-33 on bone marrow eosinophil progenitors to capture observed drops in this population, consistent with the known role of IL-33 in eosinophil proliferation and survival.

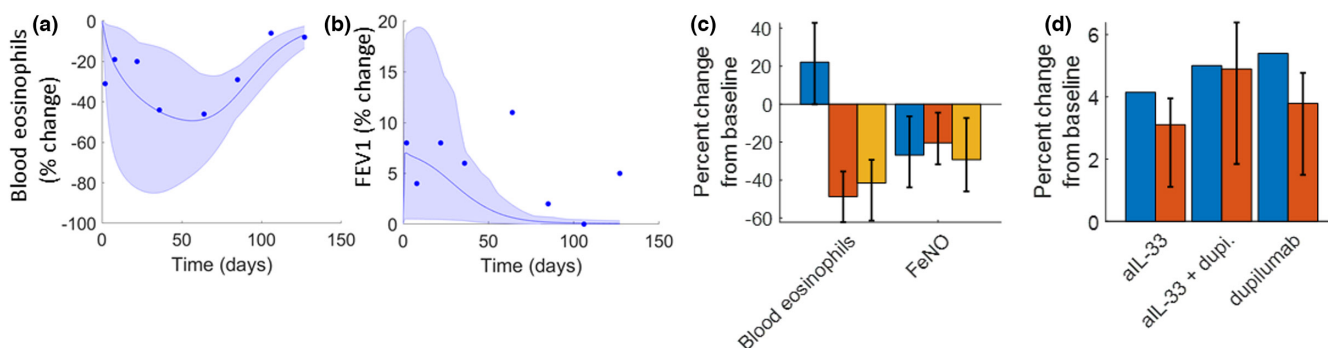


**FIGURE 5** Validation of model predictions for anti-IL-33 therapy. Simulations show predicted change from baseline for treatment with etokimab 300 mg i.v. for (a) blood eosinophils and (b) FEV1. Data are shown as blue points; simulation mean and 95% interval are shown as a blue band plot. (c) Simulation predictions of blood eosinophils and FeNO for combination anti-IL-33/anti-IL-4R $\alpha$  study for 300 mg Q2W of either anti-IL-4R $\alpha$  (blue), anti-IL-33 (red) or both anti-IL-4R $\alpha$  and anti-IL-33 (orange). Error bars show mean and middle 50% interval of simulation values. (d) Comparison of clinical (blue) and simulated (red) FEV1 improvements for anti-IL-33, anti-IL-33+ dupilumab, or dupilumab. Error bars represent the mean and middle 50% interval.

## Predictions for anti-IL-33 therapy in patients with severe asthma

To investigate IL-33/ST2 pathway inhibition, we first simulated anti-IL-33 therapy and compared results to two recent clinical studies. First, we simulated 300 mg i.v. anti-IL-33 therapy as in the etokimab phase IIa trial,<sup>26</sup> and validated predictions for FEV1 and blood eosinophils. As expected, simulated anti-IL-33 led to reduced eosinophils and increased FEV1, and showed good agreement with clinical data, see [Figure 5a,b](#).

We next simulated a phase II study of mono- and combination-therapy of anti-IL-4R $\alpha$  (dupilumab) and anti-IL-33 (REGN-3500). The study found superior response of dupilumab versus anti-IL-33 monotherapy, and no significant benefit of combination therapy over dupilumab monotherapy.<sup>27</sup> Likewise, model simulations predict that combination of anti-IL-33 and anti-IL-4R $\alpha$  is not significantly better than anti-IL-4R $\alpha$  alone for FeNO and blood eosinophils reduction, see [Figure 5c](#). Anti-IL-33 is predicted to impact both eosinophil recruitment and survival, with the net impact being a reduction in blood eosinophils. FEV1 predictions for combination and monotherapies are similar, with slightly more improvement for dupilumab or combination compared to anti-IL-33 monotherapy, suggesting little benefit for combination over anti-IL-4R $\alpha$  alone. FEV1 changes are also well captured for this population, see [Figure 5d](#) (variability not reported).

## Predictions for anti-ST2 therapy in patients with severe asthma

Following the validation of appropriate predicted responses to anti-IL-33, we next simulated the Zenyatta

phase IIb trial of anti-ST2 (astegolimab) to predict changes in clinical biomarkers. This clinical population was enriched for eosinophil low patients, and the Vpop was adjusted to the same subpopulation distribution. Simulations were performed for the study's three treatment doses: 70 mg, 210 mg, and 490 mg, s.c., Q4W for 52 weeks.

We predicted the steady-state change in blood eosinophils (Figure 6a), FeNO (Figure 6b), and FEV1 (Figure 6c), and compared them with the clinical data. Interestingly, despite accurate predictions for anti-IL-33, we observed substantial discrepancies for anti-ST2. For example, blood eosinophils decreased ~45% versus 28% at 70 mg, 46% versus 30% at 210 mg, and 47% versus 32% at 490 mg in simulations versus observed data, respectively. Mean FeNO reductions are also overpredicted compared to the clinical data: 19% versus 6%, 23% versus 2%, and 25% versus 6% for 70, 210, and 490 mg Q4W, respectively, although the clinical data are highly variable. FEV1 changes are overestimated as 2.6% versus 1.0%, 3.2% versus 2.0%, for 70 and 210 mg, respectively, whereas they are underpredicted (3.5% vs. 6.0%) 490 mg. These discrepancies reveal a less-than-expected clinical impact of the treatment on T2 pathways, whereas the FEV1 underprediction at the high dose is driven primarily by the T2 low subpopulation (see ref. 8 Supplementary Data). Taken together, these results suggest the importance of either unidentified differences between the anti-IL-33 and anti-ST2 trials populations, or non-T2 pathway effects of ST2 not captured by the QSP model.

## Predictions for anti-ST2 therapy in patients with a protective ST2 single-nucleotide polymorphism

In addition to the common variant of ST2, a variant with reduced risk of asthma has been identified.<sup>28</sup> This single-nucleotide polymorphism (SNP) shows an approximately four-fold reduction in IL-33 affinity for ST2.<sup>29</sup> We ran

simulations to explore the impact of this SNP for anti-ST2 therapy in eosinophil high and low subpopulations, see Supplementary Information (“Effect of ST2 SNP variants on anti-ST2 response”). Simulations indicate that the reduced potency lessens the influence of IL-33, thereby reducing the impact of anti-ST2, especially for blood eosinophils, see Figure S5.

## Exploration of IL-33/ST2 pathway biology

We next performed sensitivity analyses to investigate the different roles that anti-IL-33 and anti-ST2 therapy play in regulating clinical biomarkers. We analyzed the eosinophil high and low subpopulations separately to identify possible differential response. For simplicity, we divided the effects of IL-33/ST2 into two sets of pathways: axis 1 captures primarily T2 cytokine production effects, and axis 2 captures the remaining effects (see Supplementary Information for implementation details). For the sensitivity analysis, we varied the shift in IL-33 half-maximal effective concentration ( $EC_{50}$ ) induced by anti-ST2 from 0% (no effect) to 100% (nominal effect) of the “base case” value based on in vitro data, see Figure 7.

For the eosinophil high population, blood eosinophils drop by up to 46% at maximum effect on both axes (Figure 7a, top right). This drop appears to be predominantly driven by axis 2 (y axis) pathway effects, which includes ST2 effects on eosinophil progenitor proliferation and survival, suggesting a more potent role for these mechanisms in anti-ST2 compared to inhibition of T2 cytokine production. Axis 1 inhibition results in increased blood eosinophils (due to IL-4/13 recruitment effects), most prominently for weak axis 2 inhibition (moving left to right along the bottom of the graph). FEV1 increases by as much as 7.7% at maximal inhibition for both axes (base case), and appears to be determined primarily by axis 1 effects, presumably due to the impact of IL-4 and IL-13

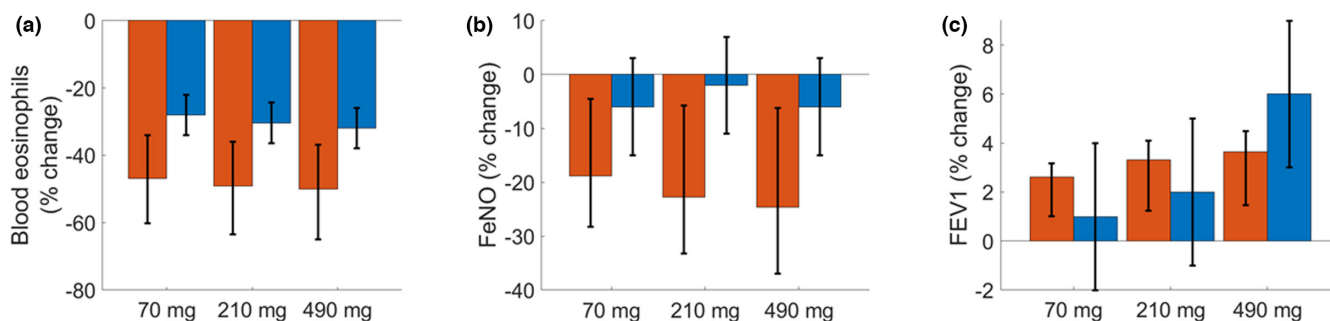


**FIGURE 6** Predicted effects of anti-ST2 therapy compared to data for the Zenyatta clinical trial. Simulations for the nominal values of ST2 inhibition are shown in red, and compared with clinical data in blue. Simulations and data show mean biomarker changes for (a) blood eosinophils, (b) FeNO, and (c) FEV1. Error bars represent the middle 50% range of the simulations and SEM for the data.

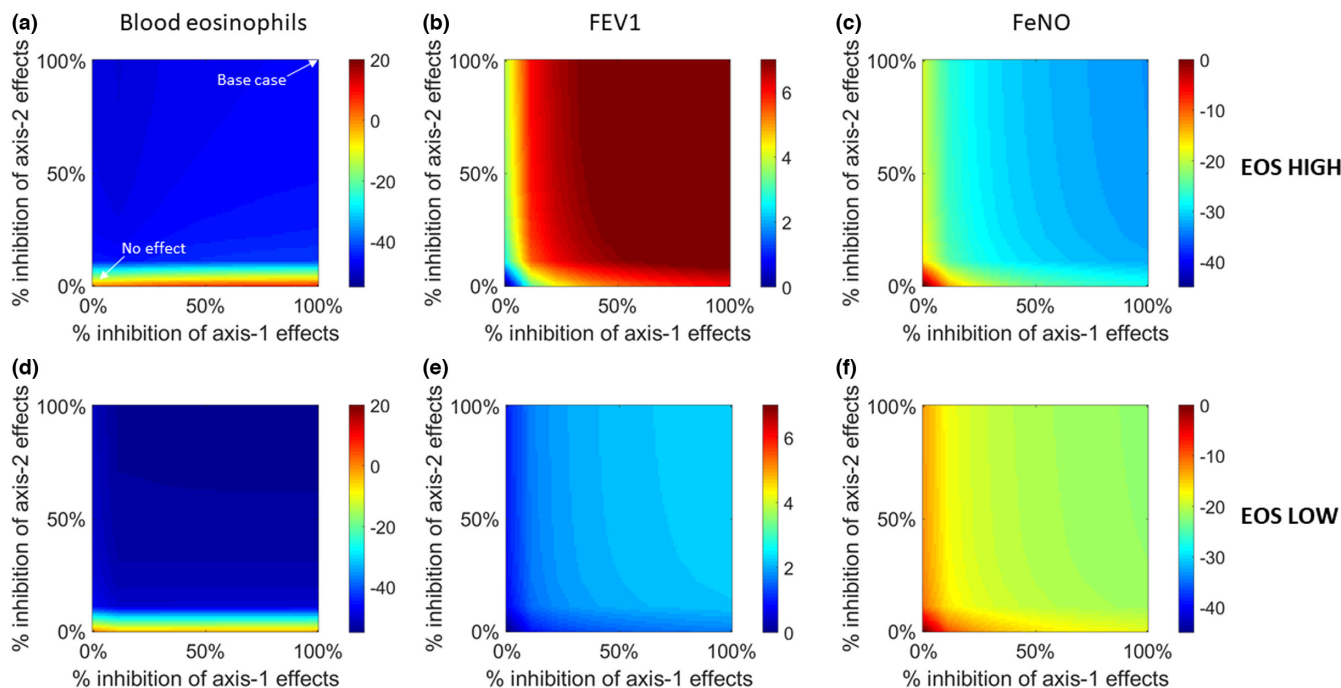


**FIGURE 7** Predicted changes in biomarkers for severe asthmatics on 490 mg Q4W s.c. of anti-ST2 as a function of anti-ST2's impact on axis-1 and axis-2 pathways. Mean changes at steady-state are shown for the eosinophil high population (top row): (a) blood eosinophils, (b) FEV1, (c) FeNO and eosinophil low population (bottom row): (d) blood eosinophils, (e) FEV1, and (f) FeNO.

effects on bronchoconstriction, see [Figure 7b](#). FeNO decreases up to 33% (base case), and is also primarily axis 1-dependent, consistent with the direct regulation of NO production by IL-4 and IL-13, see [Figure 7c](#).

As with the eosinophil high subgroup, the eosinophil low group blood shows eosinophils regulated mainly by axis 2 effects. However, increases in blood eosinophils with axis 1 inhibition are not observed ([Figure 7d](#), lower right corner), presumably due to the relatively low concentrations of T2 cytokines in this subpopulation. Interestingly, stronger maximum decreases are predicted compared to the eosinophil high group. The fewer eosinophils at baseline leads to a larger percent reduction, despite smaller absolute change in eosinophil numbers. Predicted FEV1 increases are minimal throughout, with a maximum of 2.2%, increasing primarily along axis 1, see [Figure 7e](#). In the Zenyatta trial, the eosinophil low subgroup ( $\leq 150$  cells/ $\mu$ l) showed up to 11% increase in FEV1 versus placebo at high dose, and less than 3% for other doses, whereas the eosinophil high subgroup showed no significant difference. This strong effect is not captured by the model, suggesting an additional, unknown role for T2 low pathways in driving FEV1 changes. FeNO also shows strong dependence on axis 1 effects, and drops of up to ~22% for the base case, see [Figure 7f](#). In total, the eosinophil low subgroup is predicted to show less response than the eosinophil high subgroup, across biomarkers, due to the generally lower levels of T2 cytokines downstream of IL-33 regulation.

## DISCUSSION

Asthma involves diverse mechanisms, and correspondingly a variety of pathways are targeted clinically with several more drugs in development. The model developed in this work provides a framework for integrating data from multiple interventions, capturing their impact on different clinical phenotypes. Vpops representing severe eosinophil/T2 high and low asthma were calibrated and validated for consistency with therapies targeting IL-13, IL-5, IL-4R $\alpha$ , TSLP, and IgE. These Vpops were used to explore the impact of anti-IL-33 and anti-ST2 therapy.

A key aspect of this work has been exploration of the IL-33/ST2 pathway and its effect on clinical end points. Predictions for anti-IL-33 showed good agreement for blood eosinophils, FeNO, and FEV1 versus data from anti-IL-33 and anti-IL-33/anti-IL-4R $\alpha$  combination therapy trials. Surprisingly then, simulations for anti-ST2 overpredicted biomarker changes in the phase II study of astegolimab. Interestingly, the clinical improvement was driven primarily by a subset of T2-low patients, whereas T2-high patients showed negligible improvement. This suggests the existence of unknown or non-T2-related ST2-mediated effects absent in the model. For example, IL-33 and ST2 production are represented as steady-state processes, whereas IL-33 may only be released sporadically in response to epithelial cell injury or death. Investigating such hypotheses may help resolve differences between anti-IL-33 and anti-ST2 and improve simulation agreement.



To better understand the nuanced impact of ST2 on endpoints like blood eosinophils, we used a sensitivity analysis to perform a systematic exploration of two axes of key biological effects. This suggested that (i) the direct impact of anti-ST2 on eosinophil progenitors is the dominant cause of reduced circulating eosinophils; and (ii) a direct impact of anti-ST2 therapy on T2 cytokines including IL-13 and IL-4 is necessary to drive significant changes in FEV1 and FeNO. This approach can delineate the complex relationship between ST2-driven effects, biomarker changes, and efficacy in clinical subpopulations. We further explored anti-ST2 for a protective ST2 variant, observing weaker treatment responses in these patients. Such efforts may inform future clinical study development.

Beyond IL-33/ST2, TSLP is also a promising target due to its upstream role in a range of asthma-associated pathways. IL-33 and TSLP have overlapping immune cell targets involved in T2 cytokine production and eosinophil regulation. Hence, therapies targeting these are expected to produce similar responses. Tezepelumab effectively reduced annualized asthma exacerbation rates (60–70%, versus placebo) in a phase IIb trial independently of baseline eosinophils,<sup>30</sup> and in the NAVIGATOR phase III trial,<sup>31</sup> with somewhat less benefit in the eosinophil low population. Meanwhile, anti-ST2 decreased exacerbations by 42% versus placebo in the high dose group,<sup>8</sup> with greater benefit in the eosinophil low group (51.4% reduction vs. 13.3% for the eosinophil high group). The relationship between biomarkers and exacerbations is nuanced, in particular for composite end points, such as CompEx,<sup>32</sup> and thus predictions may require advanced methods such as in a recent “repeated time-to-event” model.<sup>33</sup> Although we do not model exacerbations, the greater predicted decrease in T2 biomarkers for anti-TSLP versus anti-ST2 is consistent with the greater clinical reduction in exacerbation rates.

To our knowledge, this model represents the broadest effort to date to holistically integrate data across multiple studies of asthma. Even so, a key area for development is the explicit inclusion of non-eosinophilic mechanisms, such as IL-17 and neutrophil biology thought to play a role in T2-low asthma. These effects are currently subsumed into the model structure through calibration. Future development will continue to include approved asthma medications and those currently being investigated, with explicit representation of background therapies, such as ICSs,  $\beta_2$  agonists, and muscarinic receptor antagonists. Finally, model extension through non-mechanistic, statistical modeling may predict additional clinical features and end points, such as exacerbations, rescue medication use, symptom scores, and events associated with worsening of disease severity. Overall, this model provides a

mechanistic basis for understanding, predicting, and optimizing mechanisms of action for the next generation of asthma therapeutics.

## AUTHOR CONTRIBUTIONS

All authors wrote the manuscript. S.R., K.G., J.F., M.R., S.S., and C.S. designed the research. J.F., K.G., and S.S. performed the research. J.F., K.G., S.S., and S.R. analyzed the data.

## ACKNOWLEDGEMENTS

The authors would like to acknowledge the contributions of Vladimir Ramirez Carrozzi and Rajita Pappu in providing in vitro data for the role of IL-33 in eosinophil progenitors.

## CONFLICT OF INTEREST STATEMENT

All authors are current or former employees and/or shareholders of Genentech.

## ORCID

Justin Feigelman  <https://orcid.org/0000-0002-6296-7087>

Tracy Staton  <https://orcid.org/0000-0002-2718-9638>

David F. Choy  <https://orcid.org/0000-0003-1351-6113>

Saroja Ramanujan  <https://orcid.org/0000-0002-0909-9786>

## REFERENCES

1. Fahy JV. Type 2 inflammation in asthma-present in most, absent in many. *Nat Rev Immunol*. 2015;15(1):57-65. doi:10.1038/nri3786
2. Jacobsen EA, Ochkur SI, Lee NA, Lee JJ. Eosinophils and asthma. *Curr Allergy Asthma Rep*. 2007;7:18-26.
3. Parulekar AD, Kao CC, Diamant Z, Hanania NA. Targeting the interleukin-4 and interleukin-13 pathways in severe asthma. *Curr Opin Pulm Med*. 2018;24:50-55.
4. Bousquet J, Jeffery PK, Busse WW, Johnson M, Vignola AM. Asthma: from bronchoconstriction to airways inflammation and remodeling. *Am J Respir Crit Care Med*. 2000;161:1720-1745.
5. Fitzpatrick AM, Chipps BE, Holguin F, Woodruff PG. T2-“low” asthma: overview and management strategies. *J Allergy Clin Immunol Pract*. 2020;8:452-463.
6. Swedin L, Saarne T, Rehnberg M, et al. Patient stratification and the unmet need in asthma. *Pharmacol Ther*. 2017;169:13-34.
7. Löhning M, Stroehmann A, Coyle AJ, et al. T1/ST2 is preferentially expressed on murine Th2 cells, independent of interleukin 4, interleukin 5, and interleukin 10, and important for Th2 effector function. *Proc Natl Acad Sci USA*. 1998;95:6930-6935.
8. Steven G Kelsen M, Ioana O Agache, MD P, Weily Soong M, Elliot Israel M, Geoffrey L Chupp M, Dorothy S Cheung M, et al. Astegolimab (anti-ST2) efficacy and safety in adults with severe asthma: a randomized clinical trial. *J Allergy Clin Immunol* 2021, 148, 790, 798

9. Corren J. New targeted therapies for uncontrolled asthma. *J Allergy Clin Immunol Pract.* 2019;7:1394-1403.
10. Ramanujan S, Gadkar K, Kadambi A. Quantitative systems pharmacology: applications and adoption in drug development. In: Mager D, Kimko H, eds. *Systems Pharmacology and Pharmacodynamics*. AAPS Advances in the Pharmaceutical Sciences Series. Vol 23. Springer; 2016.
11. Karelina T, Voronova V, Demin O, Colice G, Agoram BM. A mathematical modeling approach to understanding the effect of anti-interleukin therapy on eosinophils. *CPT Pharmacometrics Syst Pharmacol.* 2016;5:608-616.
12. Karelina TA, Zhudenkov KV, Demin OO, et al. Regulation of leukotriene and 5oxoETE synthesis and the effect of 5-lipoxygenase inhibitors: a mathematical modeling approach. *BMC Syst Biol.* 2012;6:141.
13. Saunders R, Kaul H, Berair R, et al. DP 2 antagonism reduces airway smooth muscle mass in asthma by decreasing eosinophilia and myofibroblast recruitment. *Sci Transl Med.* 2019;11:1-12.
14. Lewis AK, Paterson T, Leong CC, Defranoux N, Holgate ST, Stokes CL. The roles of cells and mediators in a computer model of chronic asthma. *Int Arch Allergy Immunol.* 2001;124:282-286.
15. Rupani H, Kent BD. Using fractional exhaled nitric oxide measurement in clinical asthma management. *Chest.* 2021;161:906-917. doi:10.1016/j.chest.2021.10.015
16. Kay AB. The role of eosinophils in the pathogenesis of asthma. *Trends Mol Med.* 2005;11:148-152.
17. Hosseini I, Feigelman J, Gajjala A, et al. gQSPSim: a SimBiology-based GUI for standardized QSP model development and application. *CPT Pharmacometrics Syst Pharmacol.* 2020;9:165-176.
18. Gadkar K, Kirouac DC, Mager DE, Van Der Graaf PH, Ramanujan S. A six-stage workflow for robust application of systems pharmacology. *CPT Pharmacometrics Syst Pharmacol.* 2016;5:235-249.
19. Hanania NA, Korenblat P, Chapman KR, et al. Efficacy and safety of lebrikizumab in patients with uncontrolled asthma (LAVOLTA I and LAVOLTA II): replicate, phase 3, randomised, double-blind, placebo-controlled trials. *Lancet Respir Med.* 2016;4:781-796. doi:10.1016/S2213-2600(16)30265-X
20. Pham T-H, Ren P, Parnes JR, Griffiths JM. Tezepelumab reduces multiple key inflammatory biomarkers in patients with severe, uncontrolled asthma in the phase 2b pathway study. *Am J Respir Crit Care Med.* 2019;199:A2677.
21. Wardlaw AL. Molecular basis for selective eosinophil trafficking in asthma: a multistep paradigm. *J Allergy Clin Immunol.* 1999;104:917-926.
22. Austin CD, Gonzalez M, Ronald E, et al. A randomized, placebo-controlled trial evaluating effects of lebrikizumab on airway eosinophilic inflammation and remodelling in uncontrolled asthma (CLAVIER). *Clin Exp Allergy.* 2020;50:1342-1351.
23. Suresh V, Mih JD, George SC. Measurement of IL-13-induced iNOS-derived gas phase nitric oxide in human bronchial epithelial cells. *Am J Respir Cell Mol Biol.* 2007;37:97-104.
24. Guo FH, Erzurum SC. Characterization of inducible nitric oxide synthase expression in human airway epithelium. *Environ Health Perspect.* 1998;106:1119-1124.
25. Londei M, Kenney B, Los G, Marino MH. A phase 1 study of ANB020, an anti-IL-33 monoclonal antibody in healthy volunteers. *J Allergy Clin Immunol.* 2017;139:AB73. doi:10.1016/j.jaci.2016.12.286
26. Londei M, Officer CM. Single-dose Phase 2a trial of etokimab (anti-IL-33) in severe eosinophilic asthma. *Eur Acad Allergy Clin Immunol.* 2019. Accessed July 14, 2022. [https://www.anaptysbio.com/wp-content/uploads/Etokimab-Phase-2a-EA\\_EAACI-June-2019\\_060219\\_FINAL.pdf](https://www.anaptysbio.com/wp-content/uploads/Etokimab-Phase-2a-EA_EAACI-June-2019_060219_FINAL.pdf)
27. Wechsler ME, Ruddy MK, Pavord ID, et al. Efficacy and safety of itepekimab in patients with moderate-to-severe asthma. *N Engl J Med.* 2021;385(18):1656-1668.
28. Grotenboer NS, Ketelaar ME, Koppelman GH, Nawijn MC. Decoding asthma: translating genetic variation in IL33 and IL1RL1 into disease pathophysiology. *J Allergy Clin Immunol.* 2013;131:856-865.e9.
29. Ramirez-Carrozzi V, Dressen A, Lupardus P, Yaspan B, Pappu R. Functional analysis of protective IL1RL1 variants associated with asthma risk: to the editor. *J Allergy Clin Immunol.* 2015;135:1080-1083.e3.
30. Corren J, Parnes JR, Wang L, et al. Tezepelumab in adults with uncontrolled asthma. *N Engl J Med.* 2017;377:936-946.
31. Corren J, Bourdin A, Chupp G, et al. Efficacy of Tezepelumab in patients with severe, uncontrolled asthma grouped by baseline blood eosinophil count and fractional exhaled nitric oxide level: results from the NAVIGATOR phase 3 study. *Am J Respir Crit Care Med.* 2021;203:A1198.
32. Fuhlbrigge AL, Bengtsson T, Peterson S, et al. A novel endpoint for exacerbations in asthma to accelerate clinical development: a post-hoc analysis of randomised controlled trials. *Lancet Respir Med.* 2017;5:577-590.
33. Svensson RJ, Ribbing J, Kotani N, et al. Population repeated time-to-event analysis of exacerbations in asthma patients: a novel approach for predicting asthma exacerbations based on biomarkers, spirometry, and diaries/questionnaires. *CPT Pharmacometrics Syst Pharmacol.* 2021;10:1-15.

## SUPPORTING INFORMATION

Additional supporting information can be found online in the Supporting Information section at the end of this article.

**How to cite this article:** Gadkar K, Feigelman J, Sukumaran S, et al. Integrated systems modeling of severe asthma: Exploration of IL-33/ST2 antagonism. *CPT Pharmacometrics Syst Pharmacol.* 2022;11:1268-1277. doi:10.1002/psp4.12842